2024, 21(2): 0480-0495
https://doi.org/10.21123/bsj.2023.7685
P-ISSN: 2078-8665 - E-ISSN: 2411-7986
Baghdad Science Journal

Comparative Study of Gamma- Ray Shielding Parameters for Different Epoxy Composites

Amal A. El-Sawy *, Eman Sarwat

Nuclear and Radiological Safety Research Center, Egyptian Atomic Energy Authority
*Corresponding Author.

Received 07/09/2022, Revised 07/05/2023, Accepted 09/05/2023, Published Online First 20/07/2023, Published 01/02/2024

Abstract

In the current work various types of epoxy composites were added to concrete to enhance its effectiveness as a gamma- ray shield. Four epoxy samples of (E/clay/B4C) S1, (E/Mag/B4C) S2, (EPIL) S3 and (Ep) S4 were used in a comparative study of gamma radiation attenuation properties of these shields that calculating using Mont Carlo code (MCNP-5). Adopting Win X-com software and Artificial Neural Network (ANN), μ/ρ revealed great compliance with MCNP-5. By applying (μ/ρ) output for gamma at different energies, HVL, TVL and MFP have been also estimated. ANN technique was simulated to estimate (μ/ρ) and dose rates. According to the results, μ/ρ of all epoxy samples scored higher than standard concrete. Both S2 and S3 samples having higher values of μ/ρ, show minimum dose rate values. (μ/ρ) and RPE% values were enhanced, the concrete containing E/Mag/B4C (S2) had the best results, while the concrete containing Ep (S4) provide the worst results. The ANN prediction results take 15 sec for estimating gamma doses corresponding to seventeen shield thicknesses, while the theoretical MCNP-5 results took approximately between 7 to 10 hours for five gamma doses. ANN provides excellent predictions with a high degree of correlation depending on increasing the number of attenuation parameters used in the training process. Also, it predicts gamma dose rates for a large number of shield thicknesses that cannot be calculated theoretically in a very short time. This supports, the created epoxy composite offers good attenuation properties for many shielding applications and could be proposed as an injecting mortar for cracks in biological shields and the walls of diagnostic and radiotherapy rooms. However, further investigations are planned for different filler ratios, for comparison purposes, in order to reach optimal shielding properties.

Keywords: ANN technique, Mass attenuation coefficient (μ/ρ), MCNP-5 model, Radiation shielding, Epoxy composite, Radiation protection efficiency (RPE%).

Introduction

Today, radiation shielding is a very important component in the radiation protection field. It is applied to optimize the dose of human radiation exposure in radiation practices such as, nuclear power plants, radiation medicine, and others[1,2]. For radiation shielding materials, it is important to know the properties of these materials. Additionally, the type of radiation, its energy and the application field would all be identified when choosing the radiation shielding material. Radiation shielding is defined as

2024, 21(2): 0480-0495
https://doi.org/10.21123/bsj.2023.7685
P-ISSN: 2078-8665 - E-ISSN: 2411-7986
Baghdad Science Journal

an interaction between particles and matter through collisions and capture by atoms. The amount of the interaction depends upon the atomic number and density of the shielding material. Consequently, a study of various types of materials components is necessary for radiation shielding in order to give the highly effective characteristics for radiation attenuatn[3,4]. Wide varieties of materials are being used in radiation protection. The choice of these materials depends on the requirements, application, cost, feasibility, availability, type of radiation, etc. Always there is a necessity to advance material for shielding purposes, which can be used under severe conditions of nuclear radiation exposure and can perform as shielding material[5]. concrete is the most commonly used material for radiation shielding in most facilities because of its cheapness, its reasonable mechanical properties and its many physical attributes for an ideal shielding material for neutrons and gamma rays.

Also, the quick increase of polymeric materials consumption encourages filler incorporation; to minimize the cost, mass and size; in addition, to increasing the stiffness and strength of the composite[6]. Many researchers have prepared polymer composites with additive inorganic material to study their shielding properties. Polymeric materials such as epoxy resin owed to containing rich in hydrogen and carbon atoms, which are very effective to slow down intermediate and fast neutrons[7,8]. Composites are important and necessary materials today because of their benefits. Fillers are the most widely used additives in polymer composition. They are used in all plastics, natural and synthetic rubber and in coating. The main reason for their use is the need for cheaper materials or for improvement in some properties of the polymer matrix such as rigidity, strength and high resistance to temperature. Today environmental awareness of people is forcing industries to choose natural materials as substitutes for non -renewable materials[9]. Epoxy based composite is more suitable for use in some serve environments such as radiation shielding in medical applications and for detector shields[10]. Recently, many researchers have studied the effect of dispersed fillers in a variety of polymers, which satisfies the requirements for radiation shielding. The studied epoxy composites can be applied in radiation attenuation with different applications, for example, for shipping and storage of radionuclide materials for many mobile and stationary sources. Also, they can be used as portable radiation shielding for the walls of diagnostic and radiotherapy rooms. Besides, it might foresee applications for detector shields, neutron guides, valves, and pipes. As well, these composites could be applied as rendering/plastering mortar or even coating for shielding structures present in nuclear foundations as a possible example for the many epoxy composites' practical uses[11].

Monte Carlo simulation method (MCNP-X code) used for the investigation of radiation interaction is found less time consuming, cost effective and applicable for desired energy of radiation[12]. The general purpose of MCNP-X code is modeling to simulate the interaction of gamma- rays with matter and tracking all particles at different energies[13]. Artificial Neural Network (ANN) is a mathematical calculation model, principally, it is a black-box model and has its own boundaries. The main advantage of using an ANN system over a traditional process is that it does not require the explicit mathematical formulation of the complex nature of the fundamental process under examination[14]. When ANN is used to resolve engineering challenges, it can analyze information very quickly and can provide relevant responses even when the data being studied contains errors or is incomplete. As a result, ANN has been applied in several fields, including environmental, biological, social, computer, earth, energy, and material scientific engineering[15]. Also, it can be utilized to search for radiation sources for nuclear security[16].

The present study has the primary aim of using epoxy composites for the construction of radiation attenuation shields used for a variety of applications, as well as a mortar for developing cracks in biological concrete shields and the walls of diagnostic and radiotherapy rooms. Also, theoretical calculations have been achieved using MCNP-5 and ANN software programs to evaluate and discuss the influence of epoxy composites on the gamma radiation shielding efficiency[11].

Materials and Methods

2024, 21(2): 0480-0495
https://doi.org/10.21123/bsj.2023.7685
P-ISSN: 2078-8665 - E-ISSN: 2411-7986
Baghdad Science Journal

Radiation Attenuation Properties

There are basic quantities which determine the scattering and absorption of photons in the matter[17]. The probability of radiation interacting with a matter per unit path length is defined as the linear attenuation coefficient. It is an important quantity characterizing the penetration and diffusion of gamma-rays in a medium. Also, its magnitude depends on the incident photon energy, the atomic number and the density (ρ) of the shielding materials[10]. The linear attenuation coefficient μ (cm^{-1}) of the composite shield is termed by Eq 1:

$$I = I_o \exp^{-\mu x} \quad 1$$

Wherever, the intensity of the beam Io decreased to I after passing through a shield of thickness x, (μ/ρ) is the mass attenuation coefficient (cm^2/g), it is defined as the linear attenuation coefficient μ divided by the density of composite shield[18]. Using the Win X-COM program, the μ/ρ was calculated for some shielding materials in the 1 keV to 10 MeV energy range. It named total in addition to cross sections and partial attenuation coefficients several interaction processes (Photoelectric absorption, Compton scattering, Absorption scattering)[19], and the material's shielding performance will be improved if the μ/ρ is larger[20].

The thickness length required to attenuate the photon by 50% is denoted by the significant parameter called half value layer (HVL). The lower HVT has the best radiation shielding material in terms of thickness requirement[15]. Likewise, the thickness of the epoxy shield that reduces radiation to one- tenth of its primary intensity is known as the tenth value layer (TVL). The better shielding material has a lower value of TVL.
The two values are calculated using the following Eq 2 and are dependent on μ values[21]:

$$HVL = \ln 2/\mu \quad \text{and} \quad TVL = \ln 10/\mu \quad 2$$

Parameter of mean free path (MFP) is describing the distance of photons transportable inside the material shield between two consecutive collisions. The MFP has been derived from the linear attenuation coefficient and it can be described by Eq 3[22].

$$MFP = 1/\mu \quad 3$$

The radiation protection efficiencies can be denoted as (RPE%) and the studied shields (concrete with epoxy composites) were computed by the following Eq 4 [23].

$$RPE\% = \left(1 - \frac{I}{I_0}\right) \times 100\ \% \quad 4$$

Where I_0 is the incident beam to the detector from the gamma-ray source without any absorber, I is a transmitted beam from the sample to the detector.

Theoretical Study:

Materials and sample preparation

In the present study, standard concrete (S0) was chosen as a primary shield and four composite standard concrete by adding four different types of epoxy, (E/clay/B_4C) S1, (E/Mag/B_4C) S2, (EPIL) S3 and (Ep) S4 were investigated. samples compositions had been taken from the preceding references[11,24,25]. The standard Bisphenol-A based Epoxy resin (EP) with technical purity 95% was used to work out the composite base. (Ep) filled with certain weigh fraction of crushed magnetite (Fe_3O_4) and crushed boron carbide (B_4C). Magnetite supplied by the Nuclear Materials Authority (El Kattameya, Egypt) in the form of a fine black powder and boron carbide (B_4C) were used as composite fillers in a homogenous mixture: EP = 15 %, Mag = 75 % and B_4C = 10 %, which stands for the EP/Mag/B_4C composite[11]. While Ilmenite filler a product of (El-Nasr Phosphate Co. – Abu Galaka – Red Sea Mines – Egypt) was prepared by crushing the ore to mesh size 500 μm; certain weight of this filler was dispersed in the Epoxy formula to produce the epoxy/ilmenite (EPIlm) composite. The mixture was stirred at room temperature and degassed to allow the entrapped air to be released, then poured with great courtesy into the sample molds and left to cure. After 24 h, the samples were extruded from molds and left 7 days for ultimate cross-linking before they were shaped to the desired dimensions[24]. Also, the epoxy/clay/boron carbide nanocomposites were manufactured using an epoxy resin, SR 1500, and SD 2505 hardener filled with a commercially available nanoclay. The mixing ratio of resin/hardener was 100:33 and the formulation bases of the epoxy were

2024, 21(2): 0480-0495
https://doi.org/10.21123/bsj.2023.7685
P-ISSN: 2078-8665 - E-ISSN: 2411-7986
Baghdad Science Journal

bisphenols A and F[25]. The chemical compositions of the composite samples were presented in Table 1.

Table 1. Elemental composition of concrete and composite samples.[11,24,25]

	Sample types				
Element	**Concrete** (ρ= 2.30 g/cm^3) S0	**Ep/clay/B4C** ρ = (1.40 g/cm^3) S1	**EP/Mag/B_4C** (ρ= 2.99 g/cm^3) S2	**EPIL** (ρ= 2.71 g/cm^3) S3	**Epoxy** (ρ=1. 11 g/cm^3) S4
H	0.0100	0.0710	0.0122	0.0159	0.0660
O	0.5320	0.1010	0.2764	0.3103	0.2310
C		0.7550	0.1285	0.1410	0.6745
B		0.0390	0.0770		
N		0.0040	0.0040		0.0285
Na	0.0290		0.0073	0.0024	
Mg		0.0009	0.0023	0.0122	
Al	0.0340	0.0120		0.0115	
Si	0.3370	0.0210	0.0579	0.0313	
K			0.0005		
Ca	0.0440		0.0473	0.0040	
Mn				0.0013	
Fe	0.0140		0.3864	0.2937	
Ti				0.1698	
V				0.0014	

Monte Carlo Simulation Cede

Monte Carlo Code (MCNP-5) was used as a main tool for the implementation of this work. A source was defined in MCNP-5 data card with commands energy (ERG), types of particles (PAR), position (POS) and direction (DIR) respectively. The ^{137}Cs radioactive point source with energy 0.662 MeV and activity of 5μCi was placed in 6 cm from the detector, and a concrete shield was placed between the detector and the radioactive source. standard concrete was chosen as a primary shield and four composite standard concrete by adding four different types of epoxy composites as S1, S2, S3 and S4 in different thicknesses from 4.25 to 5.50 cm[26]. The linear and mass attenuation coefficients had been determined by computing the transmission of γ-rays through those four different compositions individually. The point detector tally F5 for the MCNP-5 had been used to calculate photon intensity and gamma dose rate. FMn card was used to convert the MCNP calculated doses (mSv/particle) to the appropriate dose rates (μSv/h). The simulation was done for 10^8 particles and the relative error was decreased to <0.005.

Artificial Neural Networks (ANNs)

Artificial neural networks (ANNs) have received much attention in recent years, and the question of which type of neural networks are better at prediction has yet to be resolved[27]. It was a set of machine learning algorithms, chart input data to output values, or classifications, by multiple layers of neurons. The outputs of each previous layer are multiplied by a weight vector, together with a bias, to create each neuron[28]. A single neuron can perform only an elementary task like multiplication and addition, yet their combination can be powerful tools for overcoming complicated tasks, like speech and image recognition, classifying complex data[29]. ANNs were effectively used for prediction, classification and association in different problem domains and they had the ability to approximate any nonlinear mathematical function, that was useful especially when the relationship between the variables was not known or was complex. One of the most popular versions of ANNs was the multilayer perceptron (MLP), a feed forward network that can use various algorithms to minimize the objective function, such as backpropagation, conjugate gradient, and other[30,31]. A simplified architecture of a MLP ANN has been presented in Fig 1. The input layer of an ANN consists of n input units with values x_i, i =1, 2,..., n, and arbitrarily computed primary weights w_i generally from the interval [-1,1]. Each

2024, 21(2): 0480-0495
https://doi.org/10.21123/bsj.2023.7685
P-ISSN: 2078-8665 - E-ISSN: 2411-7986
Baghdad Science Journal

unit in the hidden (middle) layer had received the weighted sum of all x_i values as the input. The output of the hidden layer indicated as y_c was computed by summing the inputs multiplied with their weights, in accordance to Eq 5 [31]:

$$y_c = f\sum_{i=1}^{n} w_i x_i \qquad 5$$

where,

f is the activation function that selected by the user

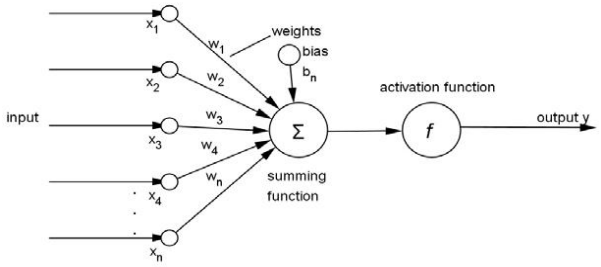

Figure 1. Schematic diagram of ANN prediction[30].

In this work, the Back Propagation Feed Forward Network (BPFFN) of the ANN technique was used in the improvement of the prediction model. The Activation Transfer Function of a back-propagation network was typically a differentiable Sigmoid (S-shape) function, which helps to apply the non-linear mapping from inputs to outputs. In this study a three layer back-propagation ANN has been used. The number of input and output neurons was determined by the nature of the problem under study. The networks were trained, tested and verified with one hidden layer and three to six neurons in the hidden layer. The output neuron (layers) has been given the predicted MCNP value which gave the best results[30].

Results and Discussion

The goal of the current study is to try finding lighter and more efficient gamma shielding epoxy that is used in the radiation field. Therefore, gamma radiation attenuation behaviors for four samples of epoxy composites have been investigated and compared with the pure concrete sample. μ and μ/ρ of the four studied samples were calculated using MCNP-5, and compared with ANN prediction and Win X-COM program.

Linear attenuation coefficients

The linear attenuation coefficient (μ) of slandered concrete So and four epoxy samples have been calculated at a photon energy of 0.05- 10 MeV and shown in Fig 2(a-c). It is clearly seen in this Fig. that the values of μ for all samples are decreasing with the energy increases. Also, (μ) of epoxy samples are decreasing rapidly and they are the same value at the low energy (0.05- 1 MeV), while they are decreasing slowly with a large difference in the high energy 1-10 MeV. For low, intermediate, and high-energy photons, the fundamental photon interaction process of the photoelectric effect, Compton scattering, and pair production can be used to explain this variation in μ, varying by the atomic number of elements of compositions. Additionally, at low photon energy, μ value of S2 and S3 are higher than So, S1 and S4, while at intermediate, and high energy, μ value of S2 are higher value than other samples. This is due to the effect of the heavy mineral Magnetite (Fe_3O_4) having density 2.99 g/cm^3, also boron has a high-density addition on S2 and S3 has a high density of Ilmenite (2.716 g/cm^3). At low energy, S2 and S3 are the best samples, while at high energy, S2 and So are the best samples.

2024, 21(2): 0480-0495
https://doi.org/10.21123/bsj.2023.7685
P-ISSN: 2078-8665 - E-ISSN: 2411-7986
Baghdad Science Journal

a) Low energy

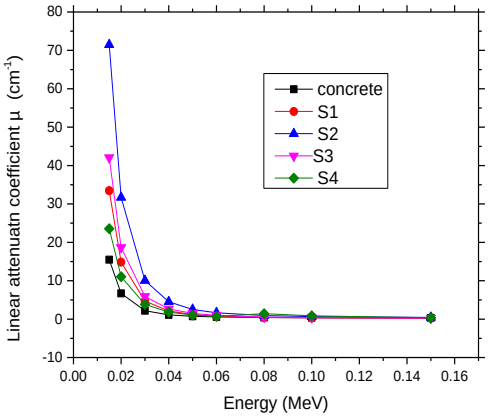

b) Intermediate energy

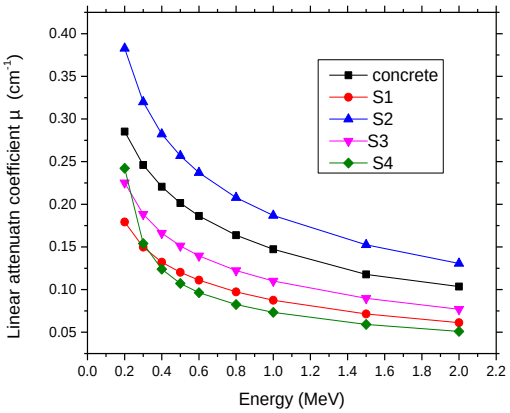

c) High energy

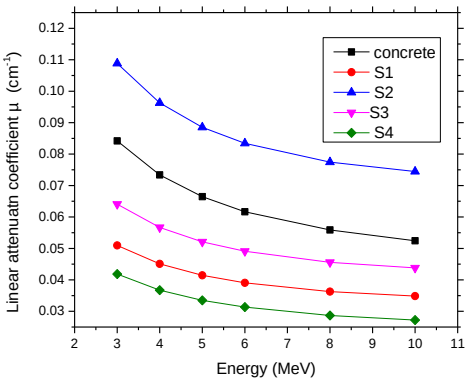

Figure 2(a-c) Linear attenuation coefficient for epoxy samples versus incident photon energy at low, intermediate and high energies.

Mass attenuation coefficient

The gamma mass attenuation coefficient (μ/ρ) value of epoxy shields at an energy range from 0.1 to 15 MeV is shown in Fig 3. It is obvious from the figure that (μ/ρ) depending on the density of the shielding materials and photon energy also; it is a related directly to the shield density and inversely proportional to the incident photon energy. The shielding efficiency of gamma radiation depends on the interaction of gamma with matter by three methods: photoelectric effect in low energy region (E < 0.8 MeV), Compton scattering in intermediate energy region (beginning 0.8 MeV to < 8 MeV), and pair production in high energy region (E > 8 MeV)[17,32]. In the Photoelectric area the μ/ρ values for the epoxy samples are rapidly decreasing with the energy increases, this decrease occurs due to the dependence of the cross section of the photoelectric absorption with the photon energy. Following in Compton region, which displays the change of μ/ρ with energy, it is noticed that μ/ρ decreases slowly with the energy increases until 6 MeV. This alteration in μ/ρ with energy in this region is perhaps associated with the dependency of the cross section of the Compton process with the atomic number (Z). Once it comes to the pair production region, it is also observed that there is a small difference of μ/ρ in the high energy (8 -15 MeV). S2 has a max. value of μ/ρ, then S3, S1, while, S4 has a min. value, the μ/ρ values increased in order as S2 > S3> S1> S4.

2024, 21(2): 0480-0495
https://doi.org/10.21123/bsj.2023.7685
P-ISSN: 2078-8665 - E-ISSN: 2411-7986
Baghdad Science Journal

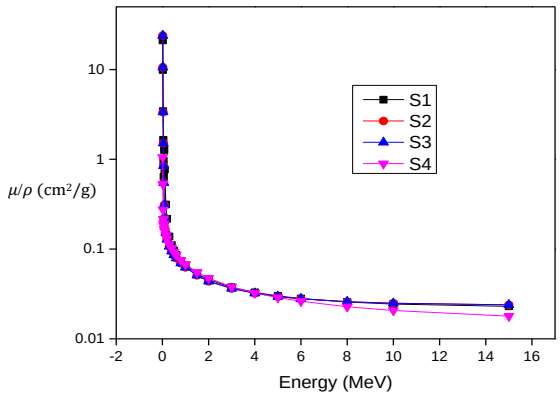

Figure 3 The variation of μ/ρ for studied epoxy at different gamma-ray energies.

Fig 4 represents the Comparison of mass attenuation coefficients μ/ρ of concrete and four epoxy samples at energy 20 MeV. This Fig displays that μ/ρ value for S1, S2 and S3 are higher than pure concrete, also, S2 and S3 are the best materials shield. While, S4 is the lowest value. This is due to the effect of heavy mineral Magnetite (Fe_3O_4) and also boron has a high-density addition on S2, and S3 has a high density of Ilmenite. While S1 and S4 have a low density and low atomic number.

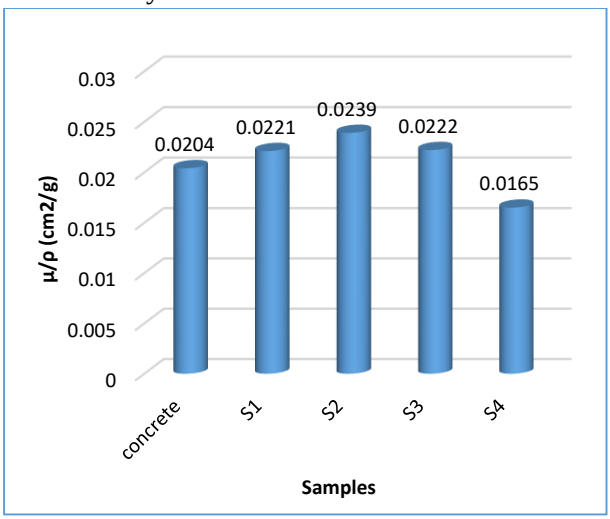

Figure 4 Comparative of μ/ρ of concrete and four samples at energy 20 MeV.

ANN Application

For the ANN simulation a program code has been written in MATLAB language. This code was used for trying different ANN architectures and the suitable model structure has been determined. In this study the parameters calculated are the mass attenuation coefficient (μ/ρ), energy, thickness and dose rate. The parameters such as thickness and energy were used as inputs in the ANN for estimation of (μ/ρ) and dose rate. μ/ρ obtained by MCNP, ANN and Win X- Com for different energies was displayed in Table 2[17]. This Table represents the comparison of (μ/ρ) of epoxy samples with MCNP-5 model, X-com program, and ANN technique at energy range (1–10 MeV). From this Table we can also observe that the values of (μ/ρ) for all samples are decreasing with the photon energy increase. Also, at low energy, S1 and S4 have a higher value while; at high energy S2 and S3 have a higher value. The (μ/ρ) values for all theoretical studies are in good agreement.

2024, 21(2): 0480-0495
https://doi.org/10.21123/bsj.2023.7685
P-ISSN: 2078-8665 - E-ISSN: 2411-7986
Baghdad Science Journal

Table 2. The μ/ρ obtained by X-Com, MCNP-5 and ANN of the Studied epoxy at different energies.

Energy (MeV)	Mass attenuation coefficient (μ/ρ)											
	EP/Clay/B_4C S1			Ep/Mag/B_4C S2			EPIL S3			EP S4		
	X-Com	MCNP-5	ANN	X-Com	MCNP-5	ANN	X-Com	MCNP-5	ANN	X-Com	MCNP-5	ANN
1	0.065	0.060	0.065	0.064	0.062	0.064	0.062	0.061	0.062	0.067	0.061	0.064
2	0.045	0.042	0.048	0.044	0.041	0.039	0.043	0.040	0.043	0.047	0.044	0.047
3	0.037	0.030	0.037	0.036	0.033	0.034	0.035	0.031	0.034	0.038	0.035	0.036
4	0.033	0.028	0.032	0.032	0.030	0.032	0.031	0.029	0.032	0.032	0.030	0.032
5	0.028	0.034	0.029	0.030	0.038	0.031	0.029	0.035	0.030	0.027	0.031	0.028
6	0.027	0.031	0.028	0.029	0.035	0.030	0.028	0.033	0.029	0.026	0.029	0.027
7	0.026	0.030	0.026	0.028	0.034	0.029	0.027	0.032	0.028	0.024	0.027	0.025
8	0.025	0.028	0.024	0.027	0.030	0.026	0.026	0.029	0.027	0.022	0.025	0.023
9	0.024	0.026	0.023	0.026	0.028	0.025	0.025	0.027	0.024	0.021	0.024	0.021
10	0.023	0.024	0.021	0.025	0.026	0.023	0.024	0.025	0.022	0.020	0.022	0.020

The relationship between X-Com and MCNP observed of μ/ρ and μ/ρ predicted by ANN is shown in Table 3. μ/ρ values decrease with the energy increasing. It also *shows the ANN* predicted (μ/ρ) values of epoxy samples for 23 values containing 10 values calculated with Win X-com and MCNP-5 at corresponding energies, from this Table, it can be observed that there are closer values for all models. The results show that the values using the three models are approximately the same.

Table 3. Prediction of μ/ρ obtained by X-Com, MCNP-5 and ANN of epoxy samples at different energies.

Energy (MeV)	Mass attenuation coefficient (μ/ρ)											
	EP/Clay/B_4C S1			Ep/Mag/B_4C S2			EPIL S3			EP S4		
	X-Com	MCNP-5	ANN	X-Com	MCNP-5	ANN	X-Com	MCNP-5	ANN	X-Com	MCNP-5	ANN
0.1			0.091			0.073			0.069			0.069
0.5			0.084			0.071			0.067			0.066
1.0	0.065	0.060	0.065	0.064	0.062	0.064	0.062	0.061	0.062	0.067	0.061	0.064
1.5			0.053			0.047			0.049			0.049
2.0	0.045	0.042	0.048	0.044	0.041	0.039	0.043	0.040	0.043	0.047	0.044	0.047
2.5			0.044			0.036			0.039			0.037
3.0	0.037	0.030	0.037	0.036	0.033	0.034	0.035	0.031	0.034	0.038	0.035	0.036
3.5			0.034			0.033			0.033			0.031
4.0	0.033	0.028	0.032	0.032	0.030	0.032	0.031	0.029	0.032	0.032	0.030	0.032
4.5			0.031			0.031			0.032			0.030
5.0	0.028	0.034	0.029	0.030	0.038	0.031	0.029	0.035	0.030	0.027	0.031	0.028
5.5			0.029			0.030			0.030			0.029
6.0	0.027	0.031	0.028	0.029	0.035	0.030	0.028	0.033	0.029	0.026	0.029	0.027
6.5			0.027			0.029			0.029			0.026
7.0	0.026	0.030	0.026	0.028	0.034	0.029	0.027	0.032	0.028	0.024	0.027	0.025
7.5			0.026			0.028			0.027			0.024
8.0	0.025	0.028	0.024	0.027	0.030	0.026	0.026	0.029	0.027	0.022	0.025	0.023
8.5			0.024			0.026			0.025			0.022
9.0	0.024	0.026	0.023	0.026	0.028	0.025	0.025	0.027	0.024	0.021	0.024	0.021
9.5			0.022			0.024			0.023			0.020
10.0	0.023	0.024	0.021	0.025	0.026	0.023	0.024	0.025	0.022	0.020	0.022	0.020
10.5			0.016			0.020			0.018			0.014
11.0			0.015			0.019			0.017			0.013

2024, 21(2): 0480-0495
https://doi.org/10.21123/bsj.2023.7685
P-ISSN: 2078-8665 - E-ISSN: 2411-7986
Baghdad Science Journal

HVL and TVL values

In order to estimate the degree of the attenuation for all studied epoxy, we usually need to calculate other parameters; half-value layer (HVL) and tenth-value layer (TVL); which were determined theoretically calculated using the Win X-Com program based on excel sheet for γ-ray energies between 0.05 and 10 MeV and the results were illustrated in Table 4. The results of these factors helped in evaluating the sample thickness required for shielding the half and tenth of the initial photon intensity. Better shielding materials are which have thinner HVL and TVL layers. Also, it is found that HVL and TVL are increasing with the energies increase; low-energy photons lose their energy at a very short distance, however, at high energy photons need a long distance to lose their energy and the values were close to one another at low energies such as at 0.05 MeV. After that, the two values gradually increased by the photon energy increases due to Photo Electric interaction. At above 0.8 MeV, they progressively increased by an increase in gamma energy, due to the process of Compton Scattering. It is clear that HVL value for all studied epoxy samples at 0.05 MeV varies between 0.62 and 2.57cm for S4 and S1 respectively, whereas at energy 10 MeV varies between 23.89 and 24.51cm for S1 and S4, respectively. Furthermore, TVL varies between 2.06 and 8.56 cm for S4 and S1, respectively at 0.05 MeV and tends to be at its highest value at 10 MeV with 79.37cm and 81.44cm for S1 and S4 respectively. From this Table we can be observed that the samples S2 and S3 possessed the thinnest HVL and TVL, while, S1 and S4 had the thickest HVL and TVL.

Table 4. HVL and TVL Values for all studied epoxy samples at energies 0.05 MeV to 10 MeV.

Energy (MeV)	HVL (cm)				TVL (cm)			
	S1	**S2**	**S3**	**S4**	**S1**	**S2**	**S3**	**S4**
0.05	2.57	0.27	0.65	0.62	8.56	0.62	2.16	2.06
0.10	2.88	1.03	1.96	0.77	10.38	0.77	6.53	2.58
0.15	3.48	1.52	2.63	1.75	11.57	1.75	8.75	5.82
0.20	3.80	1.80	3.02	2.75	12.62	2.75	10.06	9.14
0.30	4.36	2.17	3.58	4.31	14.51	4.31	11.89	14.33
0.40	4.83	2.45	4.02	5.39	16.18	5.39	13.36	17.93
0.50	5.33	2.69	4.41	6.22	17.72	6.22	14.67	20.68
0.60	5.76	2.91	4.78	6.91	19.15	6.91	15.88	22.98
0.66	5.96	2.99	4.90	7.10	19.81	7.10	16.29	23.60
0.80	6.56	3.32	5.44	8.08	21.80	8.08	18.09	26.85
1.00	7.29	3.70	6.05	9.10	24.25	9.10	20.12	30.23
1.17	8.16	4.13	6.77	10.24	27.10	10.24	22.50	34.04
1.33	8.96	4.54	7.43	11.27	29.78	11.27	24.69	37.44
2.00	10.45	5.24	8.61	13.06	34.71	13.06	28.62	43.39
3.00	13.04	6.36	10.57	15.93	43.33	15.93	35.12	52.94
4.00	15.26	7.19	12.11	18.16	50.71	18.16	40.25	60.33
5.00	17.19	7.82	13.35	19.90	57.12	19.90	44.37	66.11
6.00	18.88	8.30	14.35	21.28	62.72	21.28	47.68	70.71
7.00	20.37	8.67	15.15	22.38	67.68	22.38	50.35	74.36
8.00	21.68	8.94	15.81	23.26	72.03	23.26	52.55	77.29
9.00	22.85	9.15	16.35	23.95	75.92	23.95	54.32	79.58
10.00	23.89	9.31	16.78	24.51	79.37	24.51	55.76	81.44

Transmission

Fig 5 displays a graphical comparison of the selected samples. It is obvious that gamma-ray transmission is dependent on the linear attenuation coefficient μ and the thickness of the shield. This is actually for $I=I_o e^{-\mu x}$, the μ value is a fundamental

2024, 21(2): 0480-0495
https://doi.org/10.21123/bsj.2023.7685
P-ISSN: 2078-8665 - E-ISSN: 2411-7986
Baghdad Science Journal

factor that depends on Z of the medium's elements and incident gamma energy. Gamma- ray attenuation parameter factors (I/I_0) for different shielding materials and shield thickness from 4.25 -5.5 cm were computed using a computer program based on excel sheet for a typical 0.662 MeV photon energy. From this Fig, it can be noticed that transmission factor for all epoxy samples is decreasing with the shield thickness increases. Sample S2 has the lowest transmission for gamma ray value which varied in the range of (0.37431 to 0.28036) and S4 has the highest transmission value (0.66059 to 0.584757), this is due to S2 having the highest density and dispersion of elemental composition of composite.

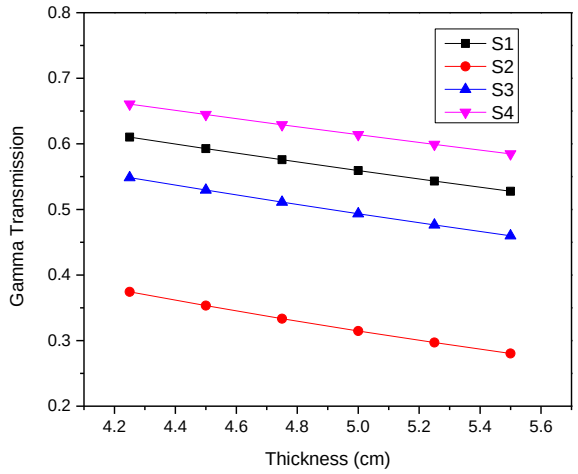

Figure 5. The variation of Transmission factor for the studied epoxy samples at different thickness.

Mean Free Path MFP

The mean free path (MFP) of the investigated epoxy composites was calculated depending on the simulation of the mass attenuation coefficient value of a gamma-ray energy range from 0.05–10 MeV. Fig 6. explain the variation of MFP versus the gamma-ray energies for all studied epoxy composites. From this Fig, it can be noticed that the MFP parameter was inversely proportional to linear attenuation coefficient, and it was increasing with the gamma energy increases. In photo-absorption region MFP values were low and the values were close to others and increased in Compton and pair-production region. The difference of MFP for the composites was depending on Z of elemental composition and densities. The highest MFP was achieved for the S4 and varied between 0.897 and 35.374 cm. While, the lowest MFP was obtained for the S2 Sample and varied between 0.394 and 13.436 cm. Therefore, it has been concluded that S2 has the best shielding among the selected various composites. The MFP values decreased in order as S2 < S3 < S1 < S4.

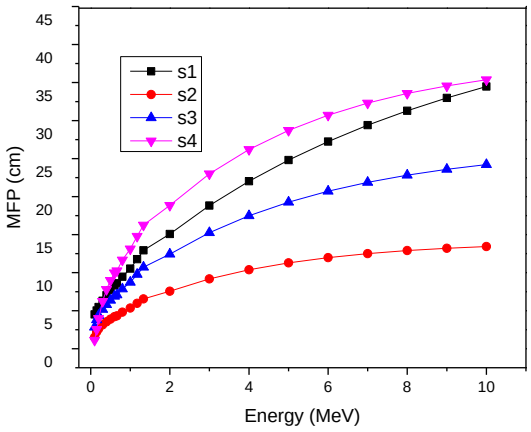

Figure 6. The variation of the MFP for all studied epoxy shield versus the gamma energy range of 0.05–10 MeV.

Gamma - ray dose rate

Fig. 7 represents the comparison of gamma- ray dose rate for the slandered concrete sample S0 and four different epoxy samples. It can be noted that the value of gamma dose rate for all epoxy samples has a lower value than concrete. Also, it can be noted that the variation of gamma dose rate for the composites was depending on Z of elemental composition and densities. Gamma dose rate value for a concrete sample which has a density (2.3 g/cm^3) was 0.808 µSv/h. The highest gamma dose rate was achieved for the S4 which has a density (1.16 g/cm^3) with a value 0.795 µSv/h. While, the lowest gamma- ray dose rate was obtained for the S2 which has a density (2.995 g/cm^3) with a value 0.776 µSv/h. Therefore, we can conclude that S2 was the best shielding between the selected various composites. Additionally, gamma- ray dose rate values decreased in order as S2 < S3 < S1 < S4, due to the effect of heavy mineral Magnetite (Fe_3O_4) and also boron on S2 which has the high-density and high attenuation of gamma ray. Composite S3 has a high density of

2024, 21(2): 0480-0495
https://doi.org/10.21123/bsj.2023.7685
P-ISSN: 2078-8665 - E-ISSN: 2411-7986
Baghdad Science Journal

Ilmenite. While S1 and S4 have a low density and low atomic number.

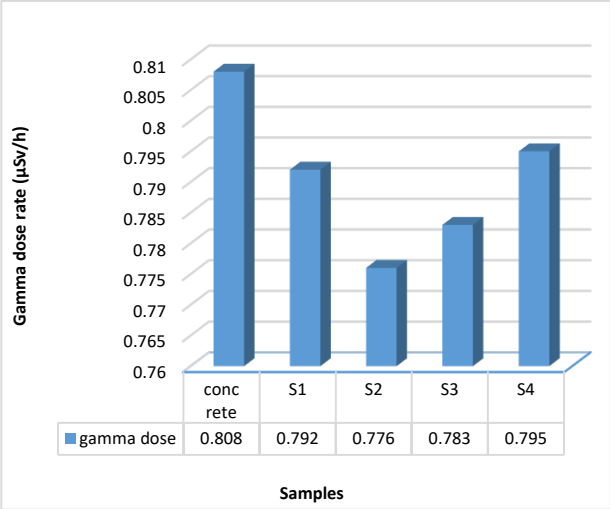

Figure. 7. Comparison of gamma-ray dose rate for concrete and four epoxy composite samples.

The variation of gamma dose rate for all studied epoxy samples against shield thickness from 4.25 cm to 5.5 cm was presented in Fig 8. From this Figure it can be noticed that S1 and S4 shields were the highest gamma dose rate values, also the min. and max. value of gamma dose rate for S1 was in the range (0.79364 to 0.72069 µSv/h) and for S4 was 0.79515 to 0.73011 µSv/h. While, samples S2 and S3 were the lowest values and the min. and max. value of gamma dose rate for S2 was in range (0.7759 to 0.64233 µSv/h) and for S3 was 0.78347 to 0.66576 µSv/h. From this Fig; we can conclude that S2 and S3 have the best materials shield, this was due to their containing boron carbide B_4C and F_2O_3 with high atomic number and density which had a good attenuator for gamma- ray, Whereas, S1 and S4 was the poorest material, this was due to they had low density.

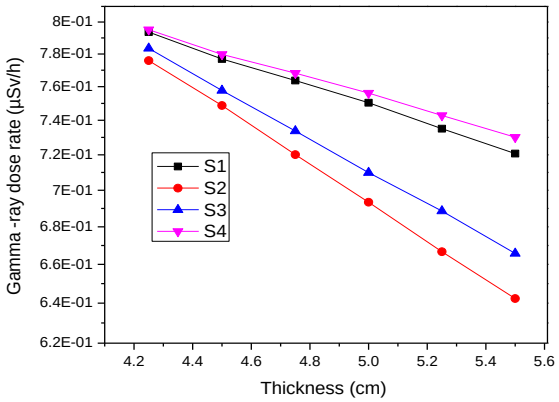

Figure. 8. Gamm - ray dose rate of epoxy composites shield with different thickness in (cm).

The relation between MCNP simulation of dose rate and predicted dose rate by ANN was shown in Table 5. This Table presents the comparison of gamma- ray dose rates between MCNP and ANN for different thicknesses from 4.25 – 5.5 cm. The output of dose rate for MCNP was considered as ANN input. The ANN was tried first to predict six outputs for dose rate. the ANN prediction values were closed for the theoretical model MCNP.

Table 5. Comparison of gamma-ray dose rate of epoxy samples calculated by MCNP-5 and ANN at Different thickness

Thickness (cm)	Gamma-ray dose rate of epoxy samples (µSv/h)							
	EP/Clay/B_4C S1		**Ep/Mag/B_4C S2**		**EPIL S3**		**EP S4**	
	MCNP-5	ANN	MCNP-5	ANN	MCNP-5	ANN	MCNP-5	ANN
4.25	0.7936	0.7834	0.7759	0.7758	0.7834	0.7854	0.7951	0.7948
4.50	0.7768	0.7769	0.7487	0.7486	0.7577	0.7580	0.7797	0.7803
4.75	0.7637	0.7581	0.7201	0.7181	0.7337	0.7274	0.7682	0.7636
5.00	0.7503	0.7503	0.6933	0.7031	0.7098	0.7098	0.7561	0.7561
5.25	0.7350	0.7351	0.6667	0.6662	0.6885	0.7009	0.7428	0.7416
5.50	0.7206	0.7205	0.6423	0.6408	0.6657	0.6659	0.7301	0.7302

2024, 21(2): 0480-0495
https://doi.org/10.21123/bsj.2023.7685
P-ISSN: 2078-8665 - E-ISSN: 2411-7986
Baghdad Science Journal

In Table 6, the ANN prediction was trained by the theoretical data given in Table 6. for six shield thicknesses as the inputs and their corresponding dose rates as outputs, then the program was asked to estimate the dose rate values for 17 shield thicknesses including the six theoretical values. The ANN results have been shown in Table 6. Additionally, the error between ANN prediction and MCNP theoretical values for six shield thickness given in Table 5 were calculated in this table. From this table it can be observed that the relative differences RD% between the MCNP-5 model and ANN prediction of (μ/ρ) values were in good agreement.

Table 6. Prediction of gamma-ray dose rate of epoxy samples calculated by MCNP-5 and ANN at different thickness.

Thickness (cm)	Gamma dose rate of epoxy samples (μSv/h)											
	EP/Clay/B_4C S1		dose rate Error	Ep/Mag/B_4C S2		dose rate Error	EPIL S3		dose rate Error	EP S4		dose rate Error
	MCNP-5	ANN		MCNP-5	ANN		MCNP-5	ANN		MCNP-5	ANN	
4.000		0.7887			0.7980			0.8158			0.8157	
4.125		0.7878			0.7943			0.8099			0.8111	
4.250	0.7936	0.7834	0.0102	0.7759	0.7758	0.0001	0.7834	0.7854	0.0020	0.7951	0.7945	0.0006
4.375		0.7789			0.7551			0.7646			0.7833	
4.500	0.7768	0.7769	0.0001	0.7487	0.7486	0.0001	0.7577	0.7580	0.0003	0.7797	0.7803	0.0006
4.625		0.7698			0.7368			0.7419			0.7742	
4.750	0.7637	0.7581	0.0056	0.7201	0.7181	0.002	0.7337	0.7274	0.0163	0.7682	0.7636	0.0046
4.875		0.7541			0.7114			0.7103			0.7597	
5.000	0.7503	0.7502	0.0001	0.6933	0.7031	0.009	0.7098	0.7097	0.0001	0.7561	0.7560	0.0001
5.125		0.7405			0.6797			0.7110			0.7467	
5.250	0.7350	0.7351	0.0001	0.6667	0.6662	0.0005	0.6885	0.7009	0.0224	0.7428	0.7416	0.0012
5.375		0.7318			0.6591			0.6880			0.7393	
5.500	0.7206	0.7205	0.0001	0.6423	0.6408	0.0015	0.6657	0.6659	0.0002	0.7301	0.7302	0.0001
5.625		0.7110			0.6300			0.6591			0.7164	
5.750		0.7091			0.6283			0.6376			0.7124	
5.875		0.7089			0.6281			0.6061			0.7119	
6.000		0.7088			0.6281			0.6060			0.7118	

Fig 9 shows a comparison between the simulated MCNP theoretical values of gamma ray dose rates for five shield thickness, and their predicted values for the 17 shield thickness doses. The results show that the error between the theoretical MCNP-5 and ANN prediction values for gamma ray dose rates was very small. Also, values using the two simulation models were approximately the same. The results have indicated that prediction using ANN is a powerful tool.

2024, 21(2): 0480-0495
https://doi.org/10.21123/bsj.2023.7685
P-ISSN: 2078-8665 - E-ISSN: 2411-7986
Baghdad Science Journal

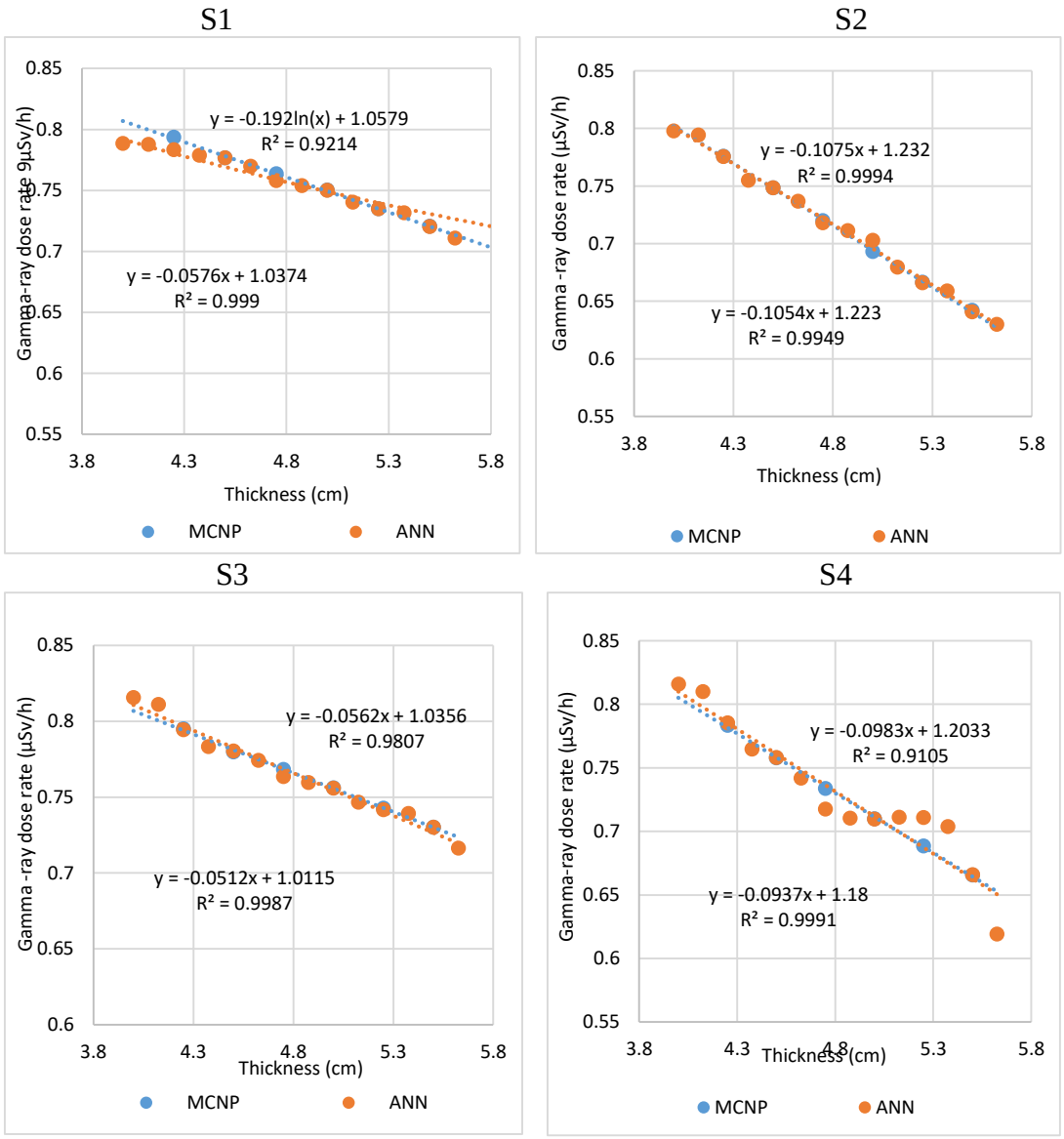

Figure 9. Comparison of gamma- ray dose rate calculated by MCNP-5 and ANN values for different shield thickness.

Radiation protection efficiency RPE %

The estimated radiation protection efficiency (RPE%) of the investigated epoxy samples at gamma energies of 0.662, 1.1732 and 1.3385 MeV were presented in Fig 9. RPE% value in the studied samples was followed by the linear attenuation coefficient. From this Figure it can be noticed that RPE% decreased with the energy increase. Additionally, it is obvious from the figure that S2 and S3 were the highest RPE % value, while, S1 and S4 were the lowest value. The RPE% values increased in order as S2 > S3> S1> S4.

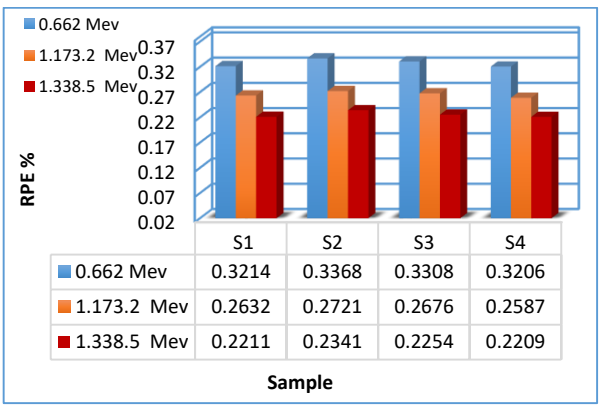

Figure. 9. Comparison of RPE% for epoxy shields at energies 0.662, 11732.2 and 1.338.5 MeV.

2024, 21(2): 0480-0495
https://doi.org/10.21123/bsj.2023.7685
P-ISSN: 2078-8665 - E-ISSN: 2411-7986
Baghdad Science Journal

Conclusion

In this research, the shielding properties of different composite materials have been investigated against gamma -ray. Studying epoxy shielding parameters such as μ, μ/ρ, HVL, TVL, MFP by the simulated model of Monte Carlo code MCNP-5, ANN technique and Win X-Com program, showed that all studied epoxy samples had a higher μ, μ/ρ than standard concrete. The S2 and S3 samples with the highest density and atomic number have been the greatest μ, μ/ρ among all samples, and minimal HVL, TVL, MFP and gamma transmissions. S2 sample was the best shielding material, while S4 was the worst. Gamma - ray dose rate for all studied samples was lower than concrete. Likewise, S2 and S3 were the best materials shield against gamma dose rate when compared to standard concrete, and RPE % for S2 sample showed the highest value while S4 was the lowest. The predicted results using ANN were almost very close to the theoretical MCNP-5 and win X-com results.

Depending on the comparison results, ANN was found a good prediction of mass attenuation coefficient and gamma-ray dose rate for shielding material. ANN was a powerful and simple alternative technique for the prediction of shielding properties. It predicts the gamma- ray dose rate for a large number of thicknesses 17 thicknesses) in 15 sec that cannot be calculated theoretically using MCNP-5 in this short time, as 6 doses of rats calculated by the model took from 7 to 10 hours. This study showed that there was an improvement in the properties of the concrete material towards the shielding of gamma-ray through the addition of epoxy composites to it.

This supports, the created epoxy composite offers good attenuation properties for many shielding applications, and could be proposed as an injecting mortar for cracks in biological shields and the walls of diagnostic and radiotherapy rooms. However, further investigations are planned for different filler ratios, for comparison purposes, in order to reach optimal shielding properties.

Author's Declaration

- Conflicts of Interest: None.
-We hereby confirm that all the Figures and Tables in the manuscript are mine ours. Besides, the Figures and images, which are not mine ours, have been given the permission for re-publication attached with the manuscript.
-Ethical Clearance: The project was approved by the local ethical committee in Nuclear and Radiological Safety Research Center, Atomic Energy Authority, Egypt.

Author's Contribution Statement

A. A. and E. S. contributed to the design and implementation of the research. A. A. collect the data of samples, design the simulation model MCNP-5 and wrote the manuscript. E. S. performed ANN simulations. All authors read and approved the final manuscript.

References

1. Mahmoudb KA, Lacomme E, Sayyed M.I, Ozpolat OF, Tashlykov OL. Investigation of the gamma ray shielding properties for polyvinyl chloride reinforced with chalcocite and hematite minerals. Heliyon 6. 2020.e03560. https://doi.org/10.1016/j.heliyon.2020.e03560
2. Mahmoud KA, Tashlykov OL, El Wakil AF, El Aassy I.E. Aggregates grain size and press rate dependence of the shielding parameters for some concretes. Prog Nucl Energy. 2020; 118: 103092. https://doi.org/10.1016/j.pnucene.2019.103092 .
3. Tekin HO, Erguzel TT, Sayyed MI, Singh VP, Manici T, Altunsoy EE, Agar O. An investigation on shielding properties of different granite samples using MCNPX code. Dig J Nanomater Bios. 2018 April- June; (13): 381 – 389.

4. 4. Ozyurt O, Altinsoy N, Karaaslan Şİ, Bora A, Buyuk B, Erk İ. Calculation of gamma ray attenuation coefficients of some granite samples using a Monte Carlo simulation code. Radiat Phys Chem. 2018; 144:271. https://doi.org/10.1016/j.radphyschem.2017.08.024.
5. Fawzy HS, Ibrahim ZH, Yasser SR, Hosam AO, Sayed FH, Eman MI, et al. Evaluation of Gamma Rays Shielding Competence for Bentonite Clay /PVA Polymer Matrix Using MCNPX Code. Arab J Nucl Sci Appl. 2020; 53(2): 177-188. http://doi.org/10.21608/ajnsa.2020.18914.1292.
6. Gheith AT, El-Sarraf MA, Kansouh WA, Eid I, Helal N, Rizk RA, et al. Determination of Mass Attenuation Coefficients, Effective Atomic Numbers and Electronic Densities for Ep and Ep/Mag/B4c Composites. Isotope Rad Res. 2017; 49(2): 255-265.
7. Chang L, Zhang Y, Liu Y, Fang J, Luan W, Yang X, et al. Preparation and characterization of tungsten/epoxy composites for γ-rays radiation shielding. Nucl Instrum Methods Phys Res B: Beam Interactions with Materials and toms. 2015; 356-357: 88-93. https://doi.org/10.1016/j.nimb.2015.04.062
8. Elmahroug Y, Tellili B and Souga C. Calculation of total mass attenuation coefficients, effective atomic numbers and effective electron density for some shielding materials. Int J Phys Res. 2013; 3: 77-86.
9. Ahmed J. Farhan, Harith I. Jaffer. Effect of water on some mechanical properties for sawdust and chopped reeds/upe composites. Baghdad Sci J. 2011; 8 (2): 551-560. https://doi.org/10.21123/bsj.2011.8.2.551-560
10. Elmahroug Y, Tellili B, Souga C. Determination of total mass attenuation coefficients, effective atomic numbers and electron densities for different shielding materials. Ann Nucl Energy. 2015; 75: 268-274. https://doi.org/10.1016/j.anucene.2014.08.015 .
11. Gheith AT, El-Sarraf MA, Hasan IE, Helal NL, Rizk RA, El- Sawy Amal A, et al. Assessment of a polymeric composite as a radiation attenuator and a restoration mortar for cracking in biological shields. Nucl Phys Energy. 2020; 21: 361-368. https://doi.org/10.15407/jnpae2020.04.361 .
12. MCNPX™ 2.4.0, RSICC Computer Code Collection. MCNPX User's Manual Version 2.4.0. Monte Carlo N- Particle Transport Code System for Multiple and High Energy Applications, Los Alamos National Laboratory, Los Alamos, New Mexico. 2002.
13. Khadem M, Mahdavi SR, Ataei G. Studying effects of gold nanoparticle on dose enhancement in megavoltage radiation. J Biomed Phys Engi. 2015; 5(4): 185-190.
14. Raju MM, Srivastava RK, Bisht Dinesh CS, Sharma HC and Kumar Anil. Development of Artificial Neural-Network-Based Models for the Simulation of Spring Discharge. Adv Artif Intell. 2011 Jan; 2(5): 1–11. https://doi.org/10.1155/2011/686258 .
15. Gencel Osman. The application of artificial neural networks technique to estimate mass attenuation coefficient of shielding barrier. Int J Phys Sci. 2009; 4 (12): 743-751.
16. Miyuki Sasaki, Yukihisa Sanada, Estiner W. Katengeza, Akio Yamamoto. New method for visualizing the dose rate distribution around the Fukushima Daiichi Nuclear Power Plant using artificial neural networks. Sci Rep. 2021; 11: 1857. https://doi.org/10.1038/s41598-021-81546-4 .
17. Abdus Sattar Mollah. Evaluation of Gamma Radiation Attenuation Characteristics of Different Type Shielding Materials used in Nuclear Medicine Services. Bangladesh J Nucl Med. 2018 July; 21(2): 108-114. https://doi.org/10.3329/bjnm.v21i2.40361 .
18. Abou Hussein EM, Madbouly AM, Ezz Eldin FM. Characterization of some radiation shielding, optical, and physical properties of fluorophosphate glasses modified by Sm3+. J Mater Sci: Mater Electron. 2021;32: 25933–25951. https://doi.org/10.1007/s10854-021-05368-w .
19. Agar O, Sayyed MI, Akman F, Tekin HO, Kaçal MR. An extensive investigation on gamma ray shielding features of Pd/Ag-based alloys. Nucl Eng Technol. 2019;51(3):853-859. https://doi.org/10.1016/j.net.2018.12.014 .
20. Gaikwad DK, Sayyed MI, Botewad SN, Obaid SS, Khattari ZY, Gawai UP, et al. Physical, structural, optical investigation and shielding features of tungsten bismuth tellurite-based glasses. J Non Cryst Solids. 2019;503e504:158e168. https://doi.org/10.1016/j.jnoncrysol.2018.09.038 .
21. Abou Hussein EM, Madbouly AM, Ezz Eldin FM. Characterization of some radiation shielding, optical, and physical properties of fluorophosphate glasses modified by Sm3+. J Mater Sci: Mater Electron. 2021. https://doi.org/10.1007/s10854-021-05368-w .
22. Mahmoud KA, Lacomme E, Sayyed MI, Ozpolat FO, Tashlykov OL. Investigation of the gamma ray shielding properties for polyvinyl chloride reinforced with chalcocite and hematite minerals. 2020; 6(3), Heliyon6:e03560. https://doi.org/10.1016/j.heliyon.2020.e03560 .
23. Yasmin S, Barua BS, Khandaker MY, Chowdhury UC, Rashid MA, Bradley DA, et al. Studies of Ionizing Radiation Shielding Effectiveness of Silica-Based Commercial Glasses Used in Bangladeshi Dwellings. Results Phys. 2018; 9: 541-549. www.journals.elsevier.com/results-in-physics

2024, 21(2): 0480-0495
https://doi.org/10.21123/bsj.2023.7685
P-ISSN: 2078-8665 - E-ISSN: 2411-7986
Baghdad Science Journal

24. El-Sarraf MA, El-Sayed Abdo A, Abdul-Wahab MA. Usability of epoxy/ilmenite composite material as an attenuator for radiation and a restoration mortar for cracks. Ann Nucl Energy. 2013; 60: 362-367. https://doi.org/10.1016/j.anucene.2013.05.016 .
25. Mahdi Rezaeian, Jamshid Kamali, Seyed Javad Ahmadi, Mohammad Amin Kiani. Effectiveness of the neutron shield nanocomposites for a dual-purpose cask of Bushehr's VVER 1000 NPP spent fuels. Nucl Eng Technol. 2017. https://doi.org/10.1016/j.net.2017.05.010 .
26. Madbouly AM, El- Sawy AA. Optimization of concrete mix with tungsten composite materials as a gamma- ray radiation shielding. Int J Sci Eng Res. 2021; 12: 1301-1315.
27. Ashour MA. Optimized Artificial Neural network models to time series. Baghdad Sci J. 2022; 19(4): 899-904. https://doi.org/10.21123/bsj.2022.19.4.0899 .
28. Matthew D, Christopher B, Azaree L. Development of a fully connected residual neural network for directional gamma ray detection. Int J Mod Phys Conf Ser. 2020; 50: 2060010. https://dx.doi.org/10.1142/S2010194520600101
29. Isaac H, Sung GS, Sang SH, Song HK, GY. A Preliminary study on dose estimator for radiation shielding using artificial regression neural network. Transactions of the Korean Nuclear Society Autumn Meeting Goyang. Korea. 2019 October; 24-25.
30. Bilmez B, Toker O, Alp S, Alp S, Oz E, Ilcelli O. A comparative study on applicability and efficiency of machine learning algorithms for modeling gamma-ray shielding behaviors. Nucl Eng Technol. 2021; 54:310-317. https://doi.org/10.1016/j.net.2021.07.031 .
31. Sarwat E, El-Shanshoury G. Estimation of air quality index by merging neural network with principal component analysis. Int J Comput Appl. 2018; 8(1): 1-12. https://doi.org/10.26808/rs.ca.v8n1.01
32. Mariyappan M, Marimuthu K, Sayyed MI, Dong MG, Kara U. Effect Bi_2O_3 on the physical, structural and radiation shielding properties of Er3+ ions doped bismuth sodium fluoroborate glasses. J Non-Cryst Solids.2018;499:75-85. https://doi.org/10.1016/j.jnoncrysol.2018.07.025 .

دراسة مقارنة لمعاملات الدروع الواقية من أشعة جاما لمركبات الإيبوكسي المختلفة

أمل عبده الصاوى ، ايمان ثروت أمين

مركز بحوث الامان النووى و الاشعاعى، هيئة الطاقة الذرية المصرية

الخلاصة

تهدف هذه الدراسة إلى تحسين أداء مادة الخرسانة كدرع واقى لأشعة جاما عن طريق إضافة بعض الأنواع المختلفة من مركبات الإيبوكسي. تم استخدام أربع عينات S1 (E /clay/ B4C) وS2 (E/ Mag / B4C) وS3 (EPIL) وS4 (Ep) للتحقيق في مقارنة خاصية التوهين الإشعاعي لهذه الدروع المحسوبة بواسطة مونت كارلو موديل (MCNP) والشبكة العصبية الاصطناعية (ANN). بالنسبة لحساب ANN، فإن المعاملات التي تم النظر فيها في الدراسة هي الجرعة الاشعاعية والسمك ومعامل التوهين(μ/ρ). تم تدريب تنبؤ ANN باستخدام النتائج النظرية أولا لسمك ستة دروع كمدخلات وμ/ρ ومعدلات الجرعة المقابلة لها كمخرجات البرنامج. بعد ذلك، تمت محاكاته لتقدير قيم معدلات الجرعة لسمك 17 درعا (بما في ذلك القيم النظرية الست) كمدخلات. كان μ/ρ لجميع عينات الإيبوكسي أعلى من الخرسانة النقية. كل من عينات S2 وS3 من خلال امتلاك قيم أعلى من μ/ρ ، تظهر قيم الحد الأدنى لمعدل الجرعة. تشير أعلى قيم μ / ρ ل S2 و S3 إلى قدرتها الأفضل على مواد التدريع ,بين جميع المركبات المختارة. تستغرق نتائج المحاكاة 15 ثانية لتقدير جرعات جاما المقابلة لسبعة عشر سمكا للتدريع، في حين استغرقت نتائج MCNP النظرية ما بين 7 إلى 10 ساعات تقريبا لخمس جرعات جاما. توفر ANN تنبؤات ممتازة بدرجة عالية من الارتباط اعتمادا على زيادة عدد خصائص التوهين المستخدمة في عملية التدريب. كما أنه يتنبأ بمعدلات جرعة أشعة جاما لعدد كبير من سمك الدروع الواقية الذي لا يمكن حسابه نظريا في وقت قصير جدا.

الكلمات المفتاحية: الشبكة العصبية الاصطناعية (ANN)، معامل التوهين (μ/ρ) ، مونت كارلو موديل(MCNP)، الدروع الواقية من الاشعاع، مركبات الإيبوكسي ، نسبة كفاءة الوقاية من الاشعاع.